Electric Power Systems Research 214 (2023) 108840

Contents lists available at ScienceDirect

Electric Power Systems Research

journal homepage: www.elsevier.com/locate/epsr

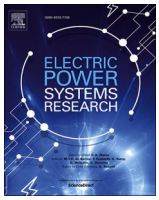

Simulation based electric stress estimation on silicone rubber polymeric insulators under multi-environmental conditions

H.P Shrimathi [a], Mithun Mondal [a], Palash Mishra [b]

[a] Department of Electrical & Electronics Engineering, Birla Institute of Technology & Sciences Pilani, Hyderabad 500078, Telangana, India
[b] Department of Electrical Engineering, National Institute of Technology, Warangal 506004, Telangana, India

ARTICLE INFO

Keywords:
Polymeric insulator
Pollution
Water droplets
Dry bands
Potential and electric field distribution

ABSTRACT

Polymeric insulators lack intermediate metal elements, resulting in non-uniform electric fields along their surface, which are further exacerbated by environmental stresses such as pollution and moisture. Researchers focused on determining the critical stresses in the polymeric insulator, paying particular attention to uniform pollution and moisture. There are, however, few studies that investigate non-uniform pollution and combinations of environmental stresses, which could influence electric field distributions. In this work, complex multi-stress environmental conditions are modeled and simulated considering pollution of different thicknesses and conductivities, water droplets of different shapes and sizes, and dry bands of varying widths and locations. This paper analyzes an 11 kV polymeric insulator's potential and electric field distribution using finite element simulations, which can be applied to any high voltage insulator under the aforementioned contaminated conditions.

1. Introduction

Polymeric insulators replace porcelain and glass insulators due to their lightweight, ease of installation, lower cost, surface hydrophobicity, and good flashover performance [1,2]. However, the electric field distribution throughout the polymeric insulator surface is non-linear due to the absence of an in-between metal part. The outdoor insulators are contaminated by natural or industrial pollution. Based on the geographical location of the insulators, pollution manifests itself as a range of types, thicknesses, and conductivities [3,4]. The inert or dry pollutants have the most negligible influence on the insulator's flashover voltage. The Silicone rubber recovers its hydrophobicity and transfers it to the pollution layer. Moisture-like fog or rainwater particles settle as droplets on a hydrophobic insulator surface [5,6]. Due to the factors like wind, rain washing, and insulator design, the contamination distribution and wetting along the insulator surface is uneven, which further aggravates the non-linear field distribution [7,8].

It has been found from [9–11] that the water droplets increase the applied electric field, resulting in partial discharges and temporal loss of hydrophobicity. Moreover, it is suggested in [12,13] that the corona onset field depends on the size and number of water droplets. The moisture interacts with the dust-like particles on the insulating surface and generates a conductive layer. When silicone rubber experience extreme humidity, it completely loses its hydrophobicity. The wet layer reduces the insulator's electrical resistance [14,15] and allows the leakage current to flow freely. As a result of uneven surface heating caused by the leakage current, a dry band arc could form, which accelerates the aging of the organic polymer material [16,17].

It is clear from earlier research that environmental stresses, such as pollution, fog, rain, and UV radiation, adversely affect the reliability of polymeric insulators [18,19]. The non-linear electric field distribution significantly impacts both the short and long-term performance of the polymer insulator. So, it is essential to analyze the E-field distribution along its surface to predict the critical high field stress regions and understand the performance of the insulator under different surface conditions. It also helps in effectively designing and applying the composite insulator.

Numerical analysis based on FEM has been used to estimate the electrical behavior of high voltage apparatus, including polymeric insulators [20,21]. The field distribution along the polymeric surface has been extensively studied in the presence of pollution and water droplets. Previous studies gave more importance to analyzing the impact of a uniform, homogeneous pollution layer [12,22]. However, it is not applicable in practice, and non-uniform contamination studies are still inadequate. Furthermore, most studies did not analyze how water droplets' form, shape, and distribution affect the discharge characteristics. Most research focuses on examining the effects of single aging stress on polymeric insulators. Electric field studies focusing on the impact of combined environmental stresses are relatively rare.

In this paper, the potential and E-field distribution along the surface of the 11 kV polymeric insulator have been comprehensively examined under uniform and non-uniform pollution conditions. Water droplets

https://doi.org/10.1016/j.epsr.2022.108840
Received 23 July 2022; Received in revised form 24 September 2022; Accepted 25 September 2022
Available online 1 October 2022

with different radii, contact angles, and shapes are modeled on clean and contaminated surface conditions. The electric field values near the water drop are determined for analysis. An electric stress investigation is also carried out in the presence of dry bands of varying lengths at various locations on a wet insulating surface. A brief overview of the different surface conditions considered in this paper for simulation studies is summarized in Fig. 1.

The remainder of the paper is structured as follows. Section 2 discusses the various considered computational models of insulators, various environmental stresses, and their simulation settings. Section 3 examines the insulator's simulated potential and electric field distribution under the effects of multi-stresses and dry bands. Section 4 concludes with the conclusions.

2. Computational Models and Simulation Settings

2.1. Insulator Profile and Material Properties

For the simulation studies, an 11 kV polymeric insulator, as shown in Fig. 2, was used as the primary goal of the proposed work is to identify the critical stress regions in the insulator under multi-stress environmental conditions that are independent of voltage level. Using EHV insulators also increases the computational complexities. The composite insulator is made up of end fittings, a fiber-reinforced plastic core (FRP), and weather sheds and shanks made of silicone rubber (SiR). The steel terminals carry the load conductors. The central FRP rod provides the necessary insulation distance between the end terminals and the required mechanical strength to support the load. In addition to shielding the FRP from environmental stresses, the SiR housing provides an adequate leakage distance along the surface of the insulator. The modeled insulator has four weather sheds with a diameter of 90 mm that are 45 mm apart and equally spaced. The red line in Fig. 2 represents the total leakage length along the insulator surface between the end fittings which is approximately 372.72 mm. The insulator's outer region is assigned as air to make the simulation model more realistic. The electrical properties such as relative permittivity ε_r and conductivity σ of different materials in the insulator model are given in Table 1 [23].

2.2. Surface Stress Conditions

Generally, the pollution severity of an insulator is determined by measuring the equivalent salt deposit density (ESDD), non-soluble deposit density (NSDD), and leakage current [25,26]. Previous experimental studies have found a strong relationship between ESDD and

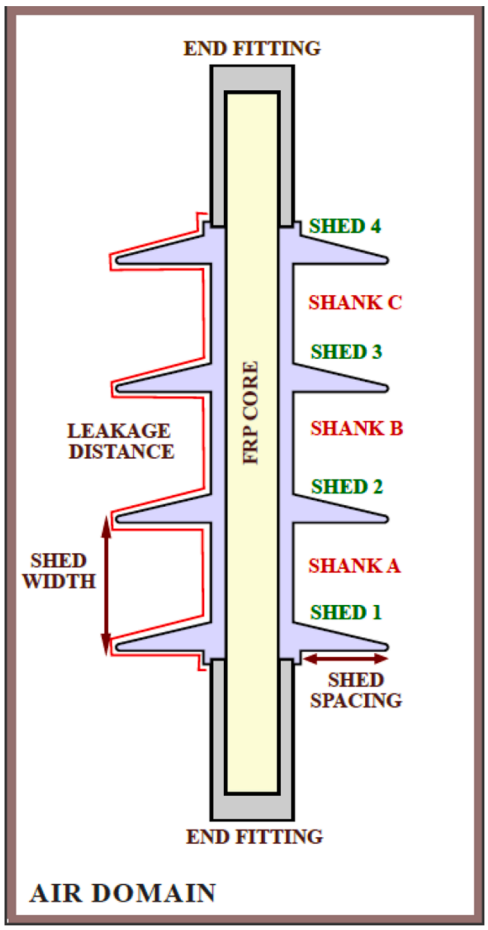

Fig. 2.. Profile of a Polymeric insulator [23].

Table 1.
Material properties of insulator model [23].

Material	Permittivity, ε_r	Conductivity, σ (S/m)
Silicone rubber	4.3	1×10^{-14}
FRP rod	7.1	1×10^{-14}
Forged steel	1	5.9×10^{7}
Air	1	1×10^{-15}

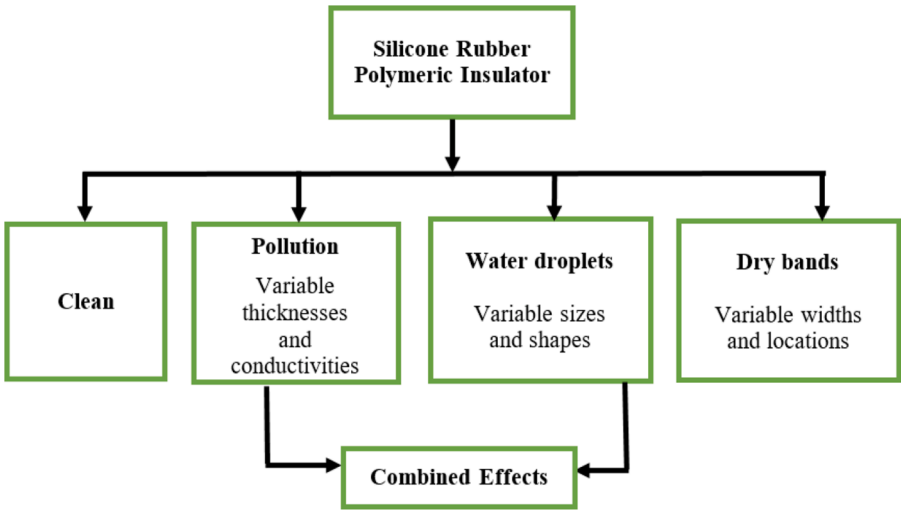

Fig. 1.. A summary of the various simulation case studies.

pollution conductivity. Various literature on the subject was thoroughly researched in order to determine the electrical properties of the external contaminants that can replicate the actual scenario and thus be used for simulation studies. The impact of environmental stresses on a polymeric insulator is investigated in this study by artificially modeling various surface conditions on the SiR housing. Table 2 provides the electrical properties such as permittivity (ε_r) and conductivity (σ) of the different considered stress conditions [12,23,24].

The following subsections explain the analysis of the various surface stresses modeled along the insulator surface.

2.2.1. Pollution

Dust particles from various sources settle on the insulator surface and completely cover it. Fog or rainwater particles diffuse into the pollution layer, forming a conductive channel. As a result, water droplets and wet layers have the same permittivity. As shown in Fig. 3a, the above effect is simulated by modeling a uniform wet pollution layer of 0.5 mm thickness [22,23,27] on the SiR housing. However, pollution deposition and wetting differ on the windward and leeward sides of the insulator string [8]. According to Ahmadi et al. [28], the contamination is not uniformly distributed on the top and bottom shed surfaces. The impact of non-uniform pollution distribution is investigated by dividing the modeled uniform wet layer into three regions and assigning different conductivities, high, medium, and low, based on contaminant accumulation and wetting, as illustrated in Fig. 3b [29,30].

2.2.2. Rain or Fog Water droplets

The surface of the silicone rubber is hydrophobic. The SiR material retains its hydrophobicity and transfers it to the overlying pollution layer. Hence, the moisture settles as discrete water drops on clean and contaminated polymeric insulators [31–33]. Even though the SiR is hydrophobic, the droplets can change their shape. The tangential electric field on the insulator surface exerts a force on the droplet and causes deformation [34,35]. The water droplets can elongate, split or coalesce with each other. For a clean new SiR surface, the contact angle of the water droplet with the polymer is 90°. It becomes zero with a layer of pollutants. But, the contact angle will return to a considerable value with time [5]. All the above findings of the previous literature are taken into account. SiR with hydrophobicity class, HC 2 and HC 3, shown in Fig. 4, are considered for this simulation study [9,12]. A total of 57 water drops, with diameters varying between 0.1 and 2 mm, semi-elliptical in shape with less than 90° contact angle, hemispherical with 90° contact angle, and with merged edges, as depicted in Fig. 5, are modeled on the insulator surface with and without pollution [27,36]. Droplets are modeled on a clean insulator surface, on the uniform and non-uniform contamination layers, as shown in Fig. 6.

2.2.3. Dry Band

The leakage current flow in a highly conductive wet layer produces heat and evaporates moisture. Due to the non-uniform current density, some insulator areas will dry out faster, resulting in the formation of dry bands [28,37]. The impact of the above condition on the electrical behavior of the polymer insulator is understood by modeling dry bands on the uniform and non-uniform wet layers. The uniform wet layer is assigned with a conductivity of 2.89×10^{-4} [38]. The HC, MC, and LC regions have the conductivities as 1×10^{-4}, 0.5×10^{-4}, and 0.1×10^{-4}, respectively. A total of 7 dry bands are modeled at various locations of SiR housing, like shanks, sheds, and near-end fittings, indicated as DB1 – DB7, as shown in Fig. 7. The modeled dry bands are of varying widths, in the range of 0.5 – 4 mm [30].

Table 2.
Electrical properties of various surface conditions [12,24].

Surface stresses	Permittivity, ε_r	Conductivity, σ (S/m)
Uniform pollution	81	6×10^{-7}
Non-uniform pollution	81	4.2×10^{-7} (HC) 3×10^{-7} (MC) 2×10^{-7} (LC)
Water droplets	81	180×10^{-6}
Dry bands	1	1×10^{-15}

2.3. Simulation Solver Settings

The voltage and electric field distributions of an 11 kV SiR insulator were calculated using 2D axisymmetric finite element simulations in COMSOL Multiphysics. Following BS EN 60815 standard, an AC voltage of 18 kV, 50 Hz, is applied to one of the end terminals while the other terminal is grounded. This applied voltage corresponds to the maximum phase-to-earth electric potential under heavy pollution conditions [24]. The primary objective of this study is to identify critical stress locations at the peak of the applied voltage at 0.005 s for one ac cycle, so the potential and electric field distributions are measured at that specific instant of time.

The E-field intensity (E) at a point is obtained by the negative gradient of the electric potential (V).

$$E = -\nabla V \tag{1}$$

The governing Eqs. (2) and (3) are considered in FEM, which allows the user to specify both the permittivity and conductivity of the material and incorporate various environmental conditions [38].

$$\nabla \cdot \left[J + \frac{\partial D}{\partial t} \right] = 0 \tag{2}$$

$$-\nabla \cdot \frac{\partial}{\partial t}(\varepsilon_0 \varepsilon_r \nabla V) - \nabla \cdot (\sigma \nabla V) = 0 \tag{3}$$

where J and $\partial D/\partial t$ are the conduction current and displacement current density, respectively. σ is the electrical conductivity, ε_0 is the dielectric constant of vacuum, and ε_r is the relative permittivity of the dielectric material. Fig. 8 shows the insulator model with increased mesh density along the critical creepage region. In the model, the element size of triangular mesh elements is manually assigned to improve the simulation accuracy.

3. Results and discussion

An 11 kV polymer insulator model is simulated under various surface conditions such as clean, pollution, water droplets, and dry band. The voltage and E-field distributions are measured along the insulator surface's creepage length (from ground to HV terminal). The results of a thorough analysis are summarised in the following subsections.

3.1. Clean Insulator

The equipotential lines are evenly distributed and pass through the insulator surface at three locations, denoted as points 1, 2, and 3 in Fig. 9a. The voltage rises gradually from the ground to the HV terminal. As shown in Fig. 9b, the electric field is strongest near the end terminals, with minor peaks seen in the shank region due to sharper edges at the intersection of weather sheds and sheaths. The E-field is tangential in the shank regions, contributing to higher field stress in those areas. Field stress is significantly lower at the shed′s tip than in the other areas. Shanks and weather sheds close to metal electrodes are subjected to more stress than intermediate ones. Because of the displacement current, the E-field is capacitive, and the results obtained are consistent with those found in the literature [22,28,39]. The clean insulator's potential and E-field distributions are used as a starting point for the analysis of other environmental stress conditions.

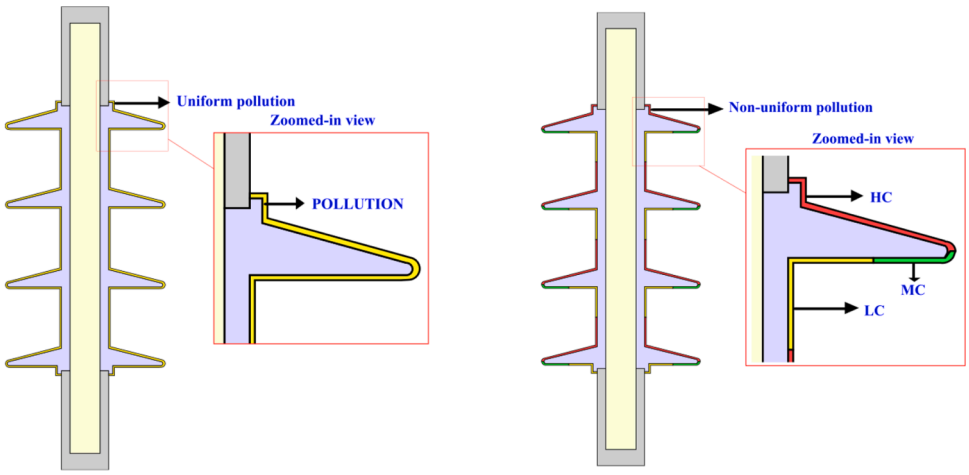

Fig. 3.. Uniform and Non-uniform pollution deposits.

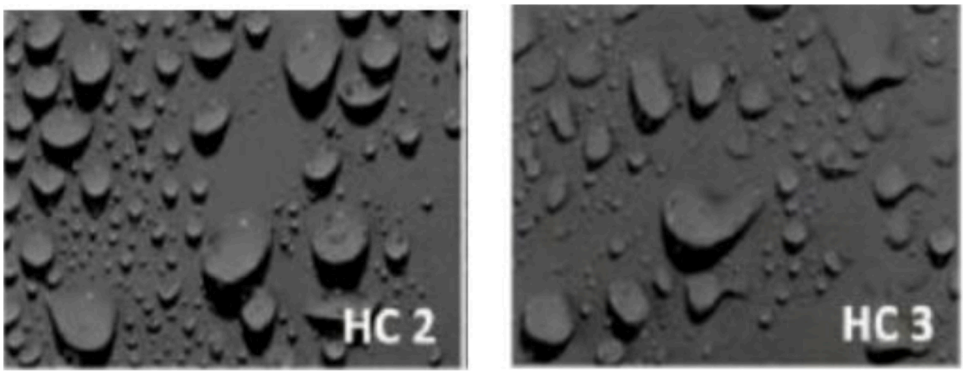

Fig. 4.. Hydrophobicity classes of insulator's surface [9].

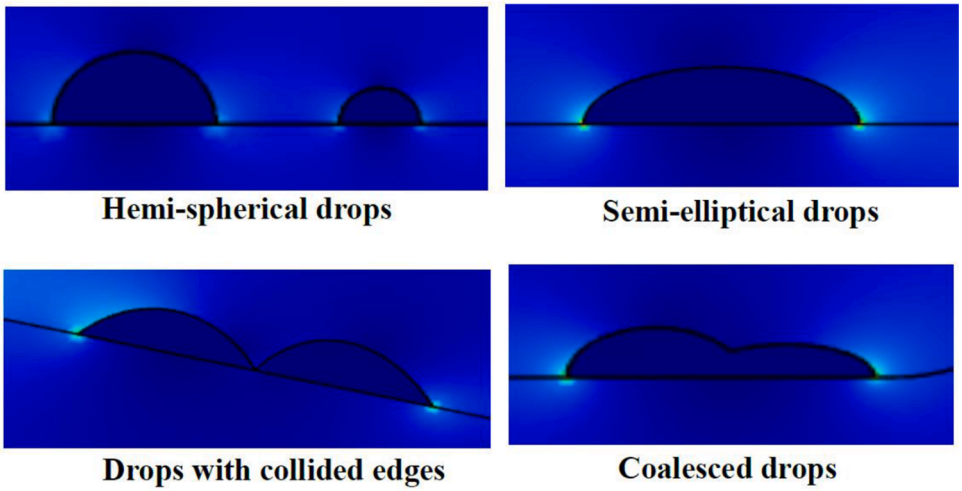

Fig. 5.. Modelled water droplets of various shapes for simulation studies.

3.2. *Uniformly Polluted Insulator*

Pollution has a significant impact on an insulator's potential and electric field distribution [22,28,40]. The equipotential lines are widely spread in the uniformly polluted insulator model and pass the insulator surface only once (indicated as point 1), whereas it passes three times in the clean insulator, as shown in the Fig. 10a. The pollution resistance smoothes the voltage distribution and reduces field stress (see Fig. 10b) along the creepage path until the leakage current flows, after which the distribution changes rapidly [23,41]. Pollution has made the field

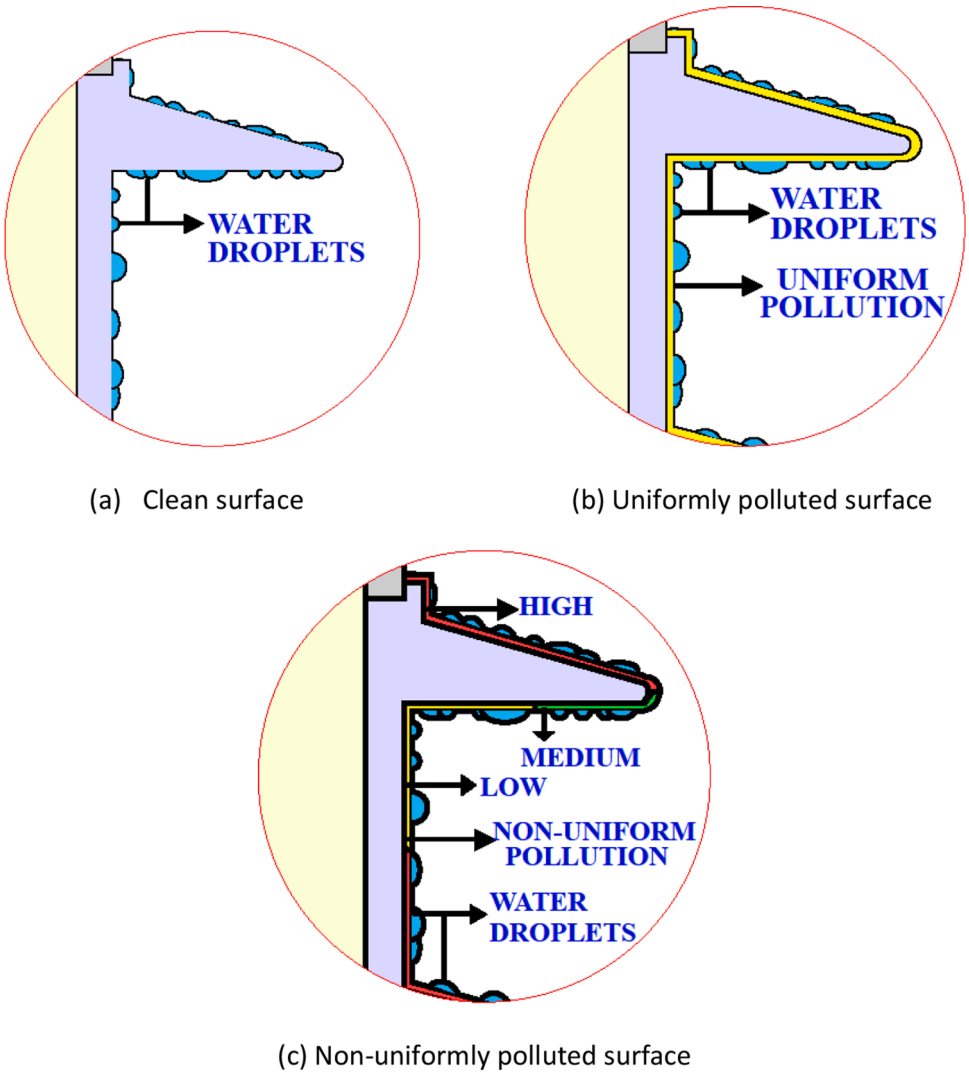

Fig. 6.. Water droplets on the insulator surface under clean and contaminated conditions.

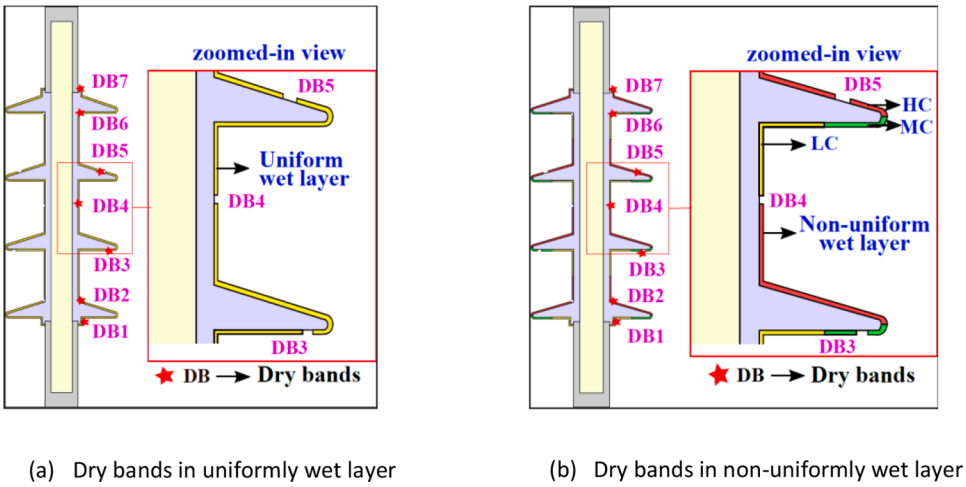

Fig. 7.. Wet layers with dry bands.

distribution uniform in the shank regions.

3.3. Non-uniformly Polluted Insulator

When the insulator surface is unevenly polluted, the equipotential lines are densely packed in low conductivity (LC) regions. However, in

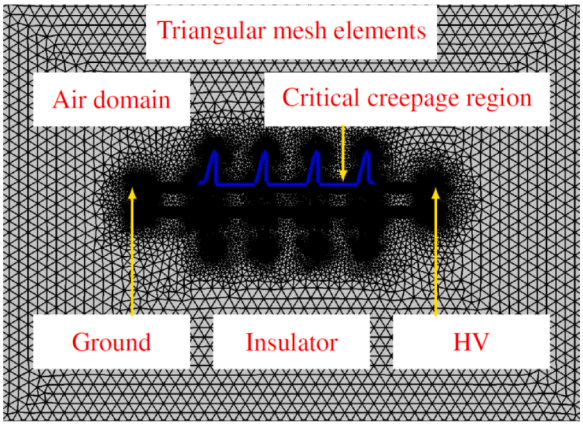

Fig. 8.. Simulation model with refined mesh elements.

the high (HC) and medium (MC) conductivity regions, the lines are far apart. In all three conductivity regions, the potential lines pass the insulator surface only once, as indicated by points 1, 2, and 3 in the 2D plot of Fig. 11a. Similar to uniform pollution, the voltage distribution is smooth, and the field stress across the insulator surface decreases. The field distribution, on the other hand, is non-uniform due to the different conductivity of the pollution layer, as shown in the Fig. 11b. Because of the non-linear relationship between surface conductivity and E-field [34,42], the LC regions are more stressed than the HC regions. This uneven field distribution could cause an electric discharge. At the shanks, the electric field is more intense due to the intersection of LC and HC pollution. As Figs. 10b and 11b show, pollution conductivities have little effect on field distribution at the sheds.

3.4. Insulator with Different Pollution Thicknesses

Heavy pollution exposure will increase its thickness on the insulator surface, and this phenomenon is investigated by varying the thickness of the uniform pollution between 0.5 mm and 2 mm while keeping its permittivity and conductivity constant [34,40]. Fig. 12 shows that as pollution thickness increases, the E-field near the end fittings decreases. As pollution accumulates, the sharpness at the intersection of shed and sheath increases, resulting in a slight rise in field magnitude. There is also an increase in E-field in the weather sheds.

3.5. Insulator with Different Pollution Conductivities

To investigate the effect of pollution conductivity on the E-field distribution of polymer insulators, the electrical conductivity (σ) of the uniform pollution is varied, keeping its thickness and permittivity constant [40,43]. Simulations were run for three different pollution conductivities, and the resulting tangential field distribution plot (shown in Fig. 13) indicates that increasing conductivity reduces E-field stress near the end terminals, and the field variation is more significant in sheds

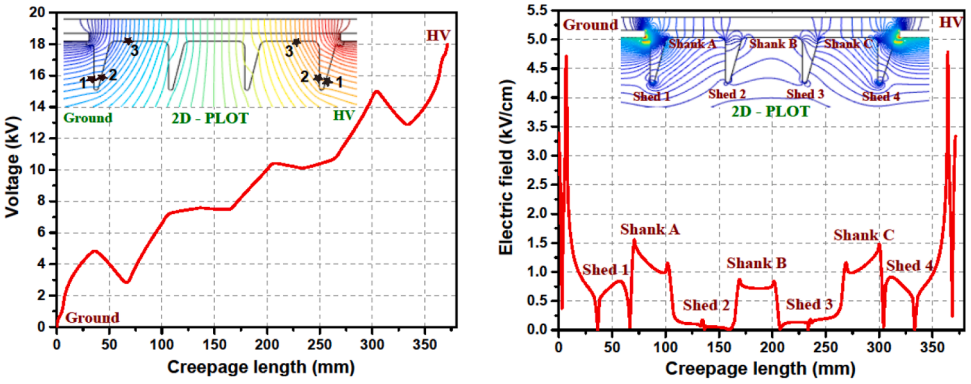

(a) Voltage distribution (b) Tangential field distribution

Fig. 9.. Potential and electric field distribution of the clean insulator.

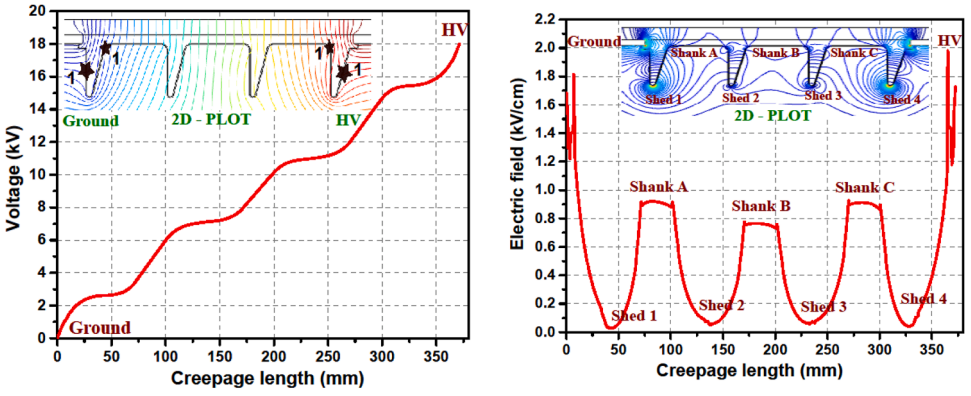

(a) Voltage distribution (b) Tangential field distribution

Fig. 10.. Polymeric insulator under uniform wet pollution condition.

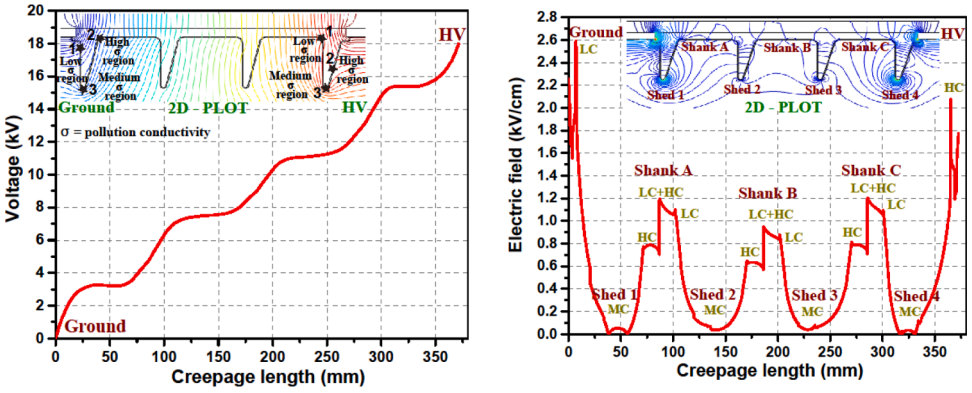

(a) Voltage distribution

(b) Tangential field distribution

Fig. 11.. Polymeric insulator under non-uniform wet pollution condition.

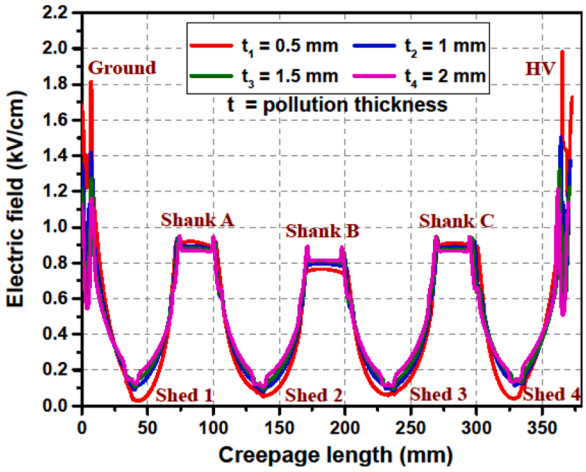

Fig. 12.. Electric field distribution under different pollution thicknesses.

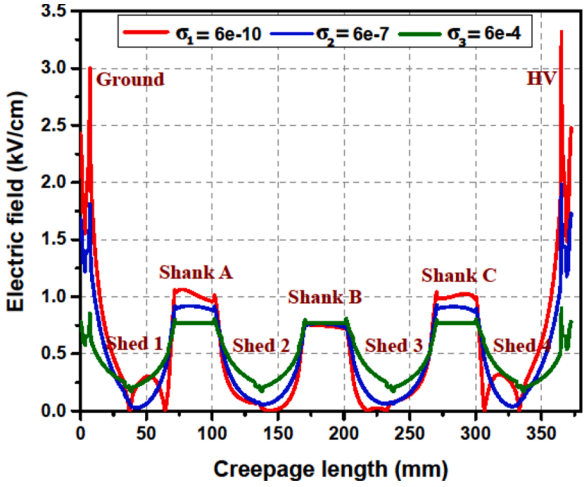

Fig. 13.. Electric field distribution under different pollution conductivities.

than in shanks. This is due to the pollution's resistance and the non-linear relationship between surface conductivity and E-field [41, 42].

3.6. Clean Insulator with Only Water Droplets

The voltage distribution is uneven, as shown in Fig. 14a, and the equipotential lines are more concentrated at the edges of the water droplets. As shown in Fig. 14b, the discrete water droplets distort the E-field distribution and increase stress at the triple points, which are the interfaces of polymer material, water drop, and air. This is because the relative permittivity of the water droplet is greater than that of silicone rubber and air [5,13]. The higher electric field concentration at the triple points can cause micro discharges between water droplets, resulting in hydrophobicity loss on the SiR surface [6]. The magnitude of the E-field at the triple points is influenced by various factors such as shape, size, contact angle, and location. Fig. 14b shows a zoomed-in view of the shank C region to demonstrate how droplet parameters affect field distribution. Numbers (1-4) represent the water droplet models on the shank surface and the corresponding E-field distribution. When water droplets of different shapes are compared, it is discovered that the maximum field magnitude occurs in coalesced water drop models. This is because increasing droplet volume reduces the distance between the droplets and the electrode, resulting in discharges [11,12]. The field stress at water droplets with smaller radii is higher than at those with larger radii. Water droplets with a lower contact angle (semi-elliptical) with the insulator surface have a higher field strength than drops with a 90° contact angle (hemispherical), which is consistent with the experimental result [9]. Droplets near end terminals and on shanks are highly distorted and subjected to higher field stress. However, the field strength at water droplets on the sheds is relatively low. The simulation results support previous research [44,45], which discovered that the presence of water droplets near the electrode reduces flashover voltage. The E-field magnitude exceeds and causes water drop corona on the sheath surface but not on the sheds, as reported in [46]. Droplets at the bottom of the shed region are subjected to higher stress than those on the top surface of the shed.

3.7. Insulator with Pollution Deposits and Water Droplets

The equipotential lines are more intense at droplet corners. However, due to pollution, they only pass through the insulator surface once, as indicated by points 1, 2, and 3 in Figs. 15a and 16a. The pollution smoothed the voltage plot, which was not smooth under only water droplet surface conditions. The electric field peaks occur at the triple point at the interface of water drop – pollution – air, but pollution reduces the intensity of the E-field at those points, as shown in Figs. 15b and 16b. Pollution conductivity affects the field stress of water droplets too. Droplets in low conductivity zones are more stressed than those in medium and high conductivity zones. Droplets with a lower contact

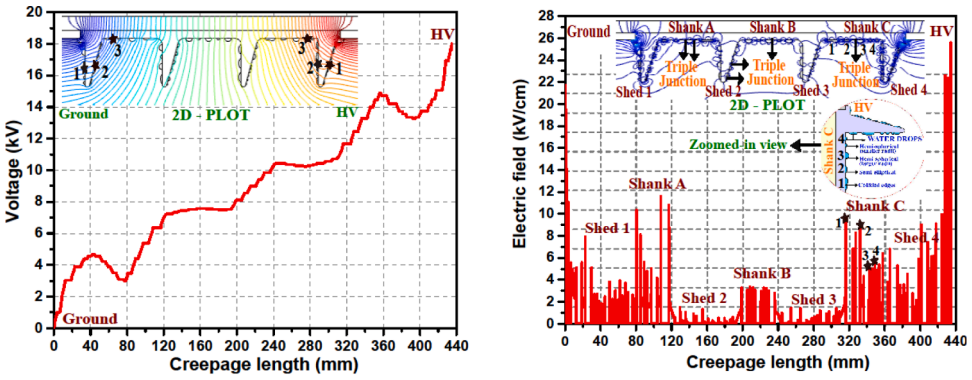

(a) Voltage distribution (b) Tangential field distribution

Fig. 14.. Clean polymeric insulator with only water droplets.

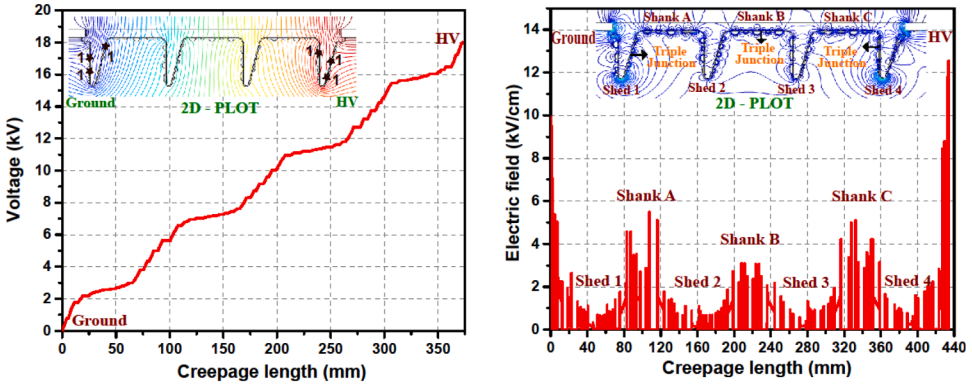

(a) Voltage distribution (b) Tangential field distribution

Fig. 15.. Polymeric insulator with uniform pollution and water droplets.

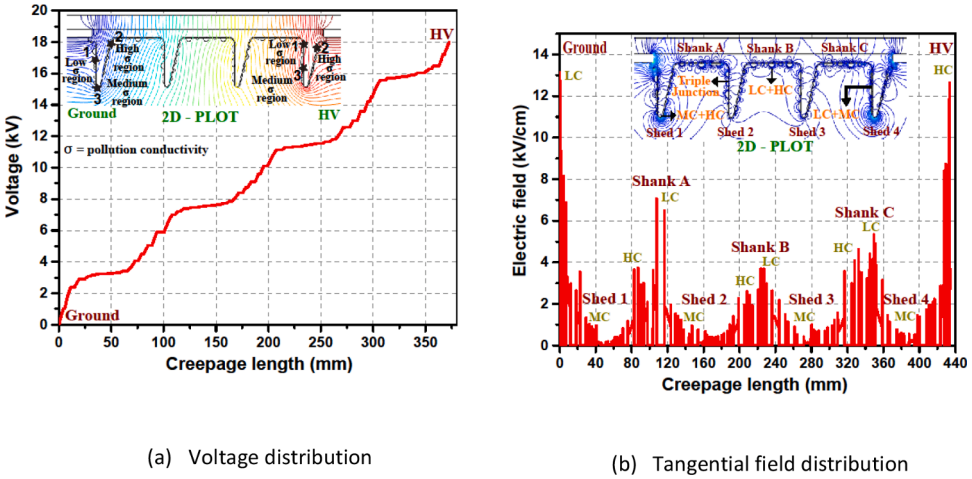

(a) Voltage distribution (b) Tangential field distribution

Fig. 16.. Polymeric insulator with non-uniform pollution and water droplets.

angle, fused edges, smaller diameters, near-end fittings, and shed-shank intersection points are highly stressed. Though the magnitude of the E-field observed at droplets under combined environmental stress conditions is less than that of the only water drops model (Fig. 14b), it is sufficient to cause partial discharges.

3.8. Insulator with Wet layers and Dry Bands

The dry bands on the polluted insulator significantly distort the voltage distribution, and the denser equipotential lines shown in Fig. 17a intensify field stress at the dry band edges (i.e., the interface of

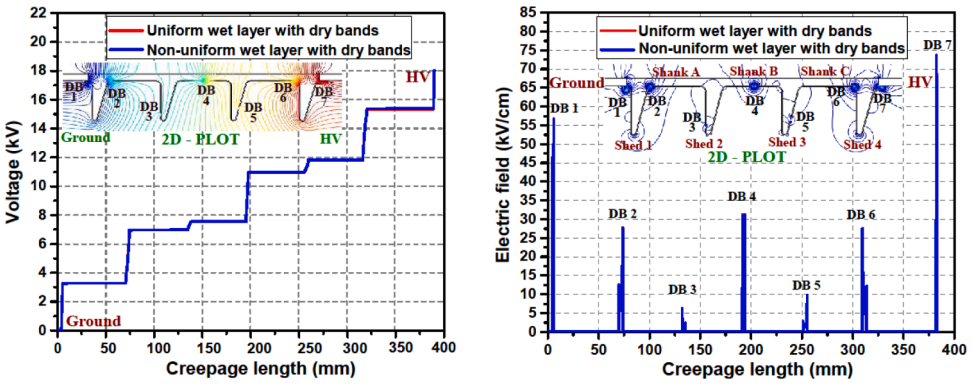

(a) Voltage distribution

(b) Tangential field distribution

Fig. 17.. Polymeric insulator with wet layers and dry bands.

the wet conductive layer and dry band), as shown in Fig. 17b. This is because dry bands act as an open circuit, interrupting the flow of leakage current and causing charge accumulation, which increases field stress [41,47–50]. The electric field intensity at the dry bands is high enough to cause an electrical breakdown and degrade the polymeric surface. Furthermore, on comparing the results of Figs. 11b and 17b, it can be inferred that pollution conductivities did not affect field strength in this case. It is observed that the location of the dry band influences the E-field magnitude, as reported by Nekahi et al. [39]. The dry bands on the shanks and near the end fittings experience higher field stress than those on the sheds. Furthermore, simulations with different sizes of dry bands were performed, and it was discovered that dry bands with smaller widths result in higher field stress, as reported in [51,52]. Table 3 provides a comparison of the main findings of this work with those of previous works.

The FEM-based simulations implemented in this research can be applied to other high-voltage devices such as cables, bushings, and surge arresters.

4. Conclusion

Simulation results show that under all surface conditions, voltage increases progressively from the ground to the HV end, with increased electric field stress at the end terminals. The shank regions are more stressed than the shed regions due to tangential electric field. The electric field stresses vary from 0.2 to 10 kV/cm in the shed region and from 0.9 to 30 kV/cm in the shank region, depending on the environmental stresses. Increased pollutant conductivity lessens the electric field in addition to slightly reducing minor field peaks at shed-shank intersections. A severe intensification of the field is evident at the edges of water droplets, where the equipotential lines are concentrated. Inside a water droplet, the field stress is zero, and shape, size, and contact angle heavily influence the field. Droplets with deformed shapes, smaller radii, and a lower contact angle experience high field stresses. Water droplet contact angles below 90 degrees result in a 2.5-fold increase in the electric field. In dry band locations, the field is powerful, and smaller width dry bands have a more significant impact on its intensity. When the dry band's width is reduced by three times, the electric stress rose by 1.5 times. The main conclusions are that the end terminals, shed-sheath intersections, water droplet edges, and dry bands are the most stressed critical regions of the insulator that lead to an electrical breakdown.

Table 3.
A comparative summary of the main findings.

Surface conditions	Previous works	This work
Clean [23,28,43]	• The field stress near the electrodes is high, and smaller field peaks occur at the intersection of the shed and shank. • The E-field is capacitive due to displacement current.	• The electric field is strongest near the end terminals, with minor peaks in the junction of weather sheds and sheaths. • The shanks are more stressed than the weather sheds.
Uniform pollution [23,28,41]	• Resistive leakage current redistributes voltage, and the E-field magnitude is less than that of a clean surface. • The flashover voltage decreases as the degree of pollution increases.	• The voltage distribution is smoothed • The electric field strength along the creepage length decreases.
Non-uniform pollution [42,43]	• The relationship between electric field strength and surface conductivity is highly non-linear.	• Low conductivity pollution regions are more stressed than high conductivity ones.
Water droplets [5,9,11–13, 44,46]	• The higher relative permittivity of water increases stress in the surrounding atmosphere. • Flashover occurs at lower voltages when droplets are close to the electrode. • The enhanced E-field causes water drop corona on the sheath surface but not in sheds. • Deformed droplets with a higher volume reduce the flashover voltage, and when the contact angle is below 90°, the E-field intensifies.	• The E-field stress rises at the triple points. • Droplets near end terminals and on shanks experience higher field stress, but droplets on the sheds experience relatively low field stress. • Droplets with coalesced edges have the highest field stress, followed by semi-elliptical and hemispherical ones.
Dry-bands with pollution [41,48, 50–52]	• Voltage concentration at the junction of the dry band and the water band increased the electric field. • Smaller-width dry bands have lesser flashover voltage. • Dry bands around the electrodes are located on a thick equipotential line, which causes a substantial voltage drop that amplifies the E-field.	• At the intersection of the wet conductive layer and dry band, the equipotential lines are denser, and the E-field stress is significantly larger. • The smaller width dry bands produce higher field stress. • Dry bands on the shanks and near the end fittings experience higher stress than those on sheds.

Authorship statement

All authors certify that they have participated sufficiently in the

work to take public responsibility for the content, including participation in the concept, design, analysis, writing, or revision of the manuscript (Eq. 1). Furthermore, each author certifies that this material or similar material has not been and will not be submitted to or published in any other publication before its appearance in the *Electric Power Systems Research*.

CRediT authorship contribution statement

Conception and design of study: H.P Shrimathi, Mithun Mondal, Palash Mishra

Acquisition of data H.P Shrimathi, Mithun Mondal

Analysis and/or interpretation of data: H.P Shrimathi, Mithun Mondal, Palash Mishra

Drafting the manuscript: H.P Shrimathi, Mithun Mondal

Declaration of Competing Interest

The authors declare that they have no known competing financial interests or personal relationships that could have appeared to influence the work reported in this paper.

Data availability

Data will be made available on request.

References

[1] J.F. Hall, History and bibliography of polymeric insulators for outdoor applications, IEEE Trans. Power Delivery 8 (1) (1993) 376–385.
[2] C. Taskforce, Polluted insulators: A review of current knowledge. CIGRE brochure, 2000.
[3] M. Farzaneh, W.A. Chisholm, Insulators for icing and polluted environments, John Wiley & Sons, 2009.
[4] B. Gao, et al., Effect of pollution non-uniformity on electric field of contaminated insulator, Insulators and Surge Arresters 3 (2008) 13–16.
[5] D. Swift, et al., Hydrophobicity transfer from silicone rubber to adhering pollutants and its effect on insulator performance, IEEE Trans. Dielectr. Electr. Insul. 13 (4) (2006) 820–829.
[6] S. Rowland, F. Lin, Stability of alternating current discharges between water drops on insulation surfaces, J. Phys. D Appl. Phys. 39 (14) (2006) 3067.
[7] Z. Zhang, et al., Study on ac flashover performance for different types of porcelain and glass insulators with non-uniform pollution, IEEE Trans. Power Delivery 28 (3) (2013) 1691–1698.
[8] Z. Zhang, et al., Investigations on ac pollution flashover performance of insulator string under different non-uniform pollution conditions, IET Generation, Transmission & Distribution 10 (2) (2016) 437–443.
[9] S. Feier-Iova, The behaviour of water drops on insulating surfaces stressed by electric field, Technische Universität, 2009. Ph.D. thesis.
[10] M. Nazemi, V. Hinrichsen, Experimental investigations on water droplet oscillation and partial discharge inception voltage on polymeric insulating surfaces under the influence of ac electric field stress, IEEE Trans. Dielectr. Electr. Insul. 20 (2) (2013) 443–453.
[11] K.K.M. Danikas, et al., Deterioration phenomena on polymeric insulating surfaces due to water droplets, J. Electr. Eng 56 (7-8) (2005) 169–175.
[12] F. Aouabed, et al., Finite element modelling of electric field and voltage distribution on a silicone insulating surface covered with water droplets, IEEE Trans. Dielectr. Electr. Insul. 25 (2) (2018) 413–420.
[13] I.J. Lopes, et al., A study of partial discharges from water droplets on a silicone rubber insulating surface, IEEE Trans. Dielectr. Electr. Insul. 8 (2) (2001) 262–268.
[14] Z. Zhang, et al., Study on the wetting process and its influencing factors of pollution deposited on different insulators based on leakage current, IEEE Trans. Power Delivery 28 (2) (2013) 678–685.
[15] R. Gorur, et al., Surface resistance measurements on non-ceramic insulators, IEEE Trans. Power Delivery 16 (4) (2001) 801–805.
[16] I. Ahmadi-Joneidi, et al., Aging evaluation of silicone rubber insulators using leakage current and flashover voltage analysis, IEEE Trans. Dielectr. Electr. Insul. 20 (1) (2013) 212–220.
[17] L. Bo, R. Gorur, Modeling flashover of ac outdoor insulators under contaminated conditions with dry band formation and arcing, IEEE Trans. Dielectr. Electr. Insul. 19 (3) (2012) 1037–1043.
[18] Z. Farhadinejad, et al., Effects of UV radiation on thermal, electrical and morphological behavior of silicone rubber insulators, IEEE Trans. Dielectr. Electr. Insul. 19 (5) (2012) 1740–1749.
[19] Y. Khan, Degradation of high voltage polymeric insulators in arid desert's simulated environmental conditions, Am. J. Eng. Appl. Sci 2 (2) (2009) 438–445.
[20] J. He, et al., Potential distribution analysis of suspended-type metal oxide surge arresters, IEEE Trans. Power Delivery 18 (4) (2003) 1214–1220.
[21] A.J. Phillips, et al., Electric fields on ac composite transmission line insulators, IEEE Trans. Power Delivery 23 (2) (2008) 823–830.
[22] A.S. Krzma, M.Y. Khamaira, Computation of the electric field and voltage distributions over the polluted surface of silicone-rubber insulators, Elixir Elec. Engg 116 (2018) 50009–50012.
[23] R. Abd-Rahman, et al., Stress control on polymeric outdoor insulators using zinc oxide microvaristor composites, IEEE Trans. Dielectr. Electr. Insul. 19 (2) (2012) 705–713.
[24] Abd Rahman, Rahisham, Investigations of ZnO microvaristor for stress control on polymeric outdoor insulators, 2012. Ph.D. thesisCardiff university.
[25] L. An, X. Jiang, Z. Han, Measurements of equivalent salt deposit density (ESDD) on a suspension insulator, IEEE Trans. Dielectr. Electr. Insul. 9 (4) (2002) 562–568.
[26] D. Maadjoudj, A. Mekhaldi, M. Teguar, Flashover process and leakage current characteristics of insulator model under desert pollution, IEEE Trans. Dielectr. Electr. Insul. 25 (6) (2018) 2296–2304.
[27] H. Shrimathi, M. Mondal, Investigation of uniform and non-uniform water droplets on different configurations of silicon rubber composite insulators subjected to ac electric field stress, in: 3rd International Conference on Energy, Power and Environment: Towards Clean Energy Technologies, 2021, pp. 1–6.
[28] I. Ahmadi-Joneidi, et al., Leakage current analysis of polymeric insulators under uniform and non-uniform pollution conditions, IET Generation, Transmission & Distribution 11 (11) (2017) 2947–2957.
[29] W. Sima, et al., Effect of non-uniform pollution on the withstand characteristics of extra high voltage (EHV) suspension ceramic insulator string, IET generation, transmission & distribution 4 (3) (2010) 445–455.
[30] H. Shrimathi, M. Mondal, Electroquasistatic simulations of wet-dry band polymeric insulator with different field grading ZnO microvaristor designs, in: IEEE 5th International Conference on Condition Assessment Techniques in Electrical Systems (CATCON), 2021, pp. 113–118.
[31] T. CIGRE, 255: Material properties for non-ceramic outdoor insulation, State of the art, CIGRE WG D 1 (2004) 14.
[32] R. Chakraborty, B.S. Reddy, Studies on high temperature vulcanized silicone rubber insulators under arid climatic aging, IEEE Trans. Dielectr. Electr. Insul. 24 (3) (2017) 1751–1760.
[33] R. Chakraborty, et al., Performance of silicone rubber insulators under thermal and electrical stress, IEEE Trans. Ind. Appl. 53 (3) (2017) 2446–2454.
[34] E.-S.M. El-Refaie, et al., Electric field distribution of optimized composite insulator profiles under different pollution conditions, Ain Shams Engineering Journal 9 (4) (2018) 1349–1356.
[35] A. Krivda, D. Birtwhistle, Breakdown between water drops on wet polymer surfaces, in: Annual Report Conference on Electrical Insulation and Dielectric Phenomena, 2001, pp. 572–580.
[36] H. Shrimathi, M. Mondal, Electric stress minimization in outdoor contaminated polymeric insulators using an appropriate field grading material, in: IEEE 18th India Council International Conference (INDICON), 2021, pp. 1–6.
[37] A. Das, et al., Electric stress analysis of a contaminated polymeric insulating surface in presence of dry bands, International Conference on Intelligent Control Power and Instrumentation (ICICPI) (2016) 89–92.
[38] K. Vaisakh, et al., Design optimization of polymeric insulators under various environmental conditions, in: IEEE 5th International Conference on Condition Assessment Techniques in Electrical Systems (CATCON), 2021, pp. 053–057.
[39] A. Nekahi, et al., Effect of pollution severity and dry band location on the flashover characteristics of silicone rubber surfaces, Electrical Engineering 99 (3) (2017) 1053–1063.
[40] H. Shrimathi, M. Mondal, Electric field and potential distribution evaluation of environmentally polluted 11 kV polymeric outdoor insulators, in: 1st International Conference on Power Electronics and Energy (ICPEE), 2021, pp. 1–6.
[41] D. Williams, et al., Formation and characterization of dry bands in clean fog on polluted insulators, IEEE Trans. Dielectr. Electr. Insul. 6 (5) (1999) 724–731.
[42] Krystian Leonard Chrzan, Federico Moro, Concentrated discharges and dry bands on polluted outdoor insulators, IEEE Trans. Power Delivery 22 (1) (2006) 466–471.
[43] P. Bala, et al., Electric stress analysis of a 11 kV RTV silicone rubber coated porcelain insulator, in: 2016 Biennial International Conference on Power and Energy Systems: Towards Sustainable Energy (PESTSE), 2016, pp. 1–6.
[44] M.G. Danikas, et al., Analysis of polymer surface modifications due to discharges initiated by water droplets under high electric fields, International Journal of Materials and Metallurgical Engineering 3 (2) (2009) 116–121.
[45] Y. Yan, et al., Study of discharge process and characteristics of discrete water droplets on the RTV hydrophobic surface in the non-uniform electric field, International Conference on Power System Technology (2006) 1–6.
[46] A. Phillips, et al., Water drop corona effects on full-scale 500 kV non-ceramic insulators, IEEE Trans. Power Delivery 14 (1) (1999) 258–265.
[47] I.J. Lopes, et al., A method for detecting the transition from corona from water droplets to dry-band arcing on silicone rubber insulators, IEEE Trans. Dielectr. Electr. Insul. 9 (6) (2002) 964–971.
[48] J.-b. Zhou, et al., Dry band formation and its influence on electric field distribution along polluted insulator, Asia-Pacific Power and Energy Engineering Conference (2010) 1–5.
[49] M.M. Hussain, et al., Dry band formation on HV insulators polluted with different salt mixtures, IEEE Conference on Electrical Insulation and Dielectric Phenomena (CEIDP) (2015) 201–204.

[50] X. Wu, et al., Research on flashover characteristics of" dry band-water band" on hydrophobic surface, CSEE Journal of Power and Energy Systems (2020).
[51] A. Nekahi, et al., Influence of dry band width and location on flashover characteristics of silicone rubber insulators, IEEE Electrical Insulation Conference (EIC) (2016) 73–76.
[52] J. He, et al., Modeling of dry band formation and arcing processes on the polluted composite insulator surface, Energies 12 (20) (2019) 3905.